

**Electronic Supplementary Information**

**Laser-induced Fe<sub>3</sub>O<sub>4</sub>-Graphene Nanozyme for  
Catalytic–Photothermal Synergetic Bactericidal Application**

Limin Yang, Liuying Chen, Zhiliang Feng, Haiyan Shi, Baokun Wang, Wenjie Liu,

Xiaojuan Liu, Ting Hou, Lei Ge,\* and Feng Li\*

College of Chemistry and Pharmaceutical Sciences, Qingdao Agricultural University, Qingdao,  
266109, People's Republic of China

\*Corresponding author: Feng Li, Lei Ge

E-mail: [lifeng@qau.edu.cn](mailto:lifeng@qau.edu.cn); [lge@qau.edu.cn](mailto:lge@qau.edu.cn)

Telephone: +86-532-58957855

## Materials and method

### 1. Reagents and materials

FeCl<sub>3</sub>, 3,3',5,5'-tetramethylbenzidine (TMB), methylene blue (MB), glutathione (GSH), 5,5'-dithiobis(2-nitrobenzoic acid) (DTNB), and hydrogen peroxide (H<sub>2</sub>O<sub>2</sub>) were supplied by Sigma-Aldrich. Kapton polyimide (PI) sheet (500HN, thickness: 125 μm) were purchased from DuPont. Prior to use, the PI sheets were ultrasonically cleaned in acetone, ethanol, and water, respectively, for 30 min each, followed by washing copiously with ultrapure water and blown dry under a stream of N<sub>2</sub> gas. Unless other indicated, all the chemicals used were of analytical reagent grade or above and used without further purification. All solutions were prepared using ultra-pure water (resistivity of 18.2 MΩ cm<sup>-1</sup> at 25 °C), which was obtained from a Milli-Q water purification system (Millipore Corp., Bedford, MA, USA).

### 2. Fabrication of LIFeG nanozyme

Briefly, the fabrication process starts with the preparation of LIG patterns on commercial polyimide sheet by computer-controlled straightforward CO<sub>2</sub> laser (10.6 μm) scanning under ambient conditions using a 40 W consumer-grade laser cutting machine (Epilog Laser MINI). The cleaned polyimide sheet was laser-scanned directly under the raster mode with 1200 dots per inch (DPI) following a designed circle patterns (diameter of 8.0 mm) array in computer at a scanning speed of 166 mm/s and laser power of 2.4 W. Subsequently, 50 μM FeCl<sub>3</sub> was prepared in ultrapure H<sub>2</sub>O under continuous magnetic stirring with pH adjusted to 2 using 1.0 M HCl solution at room temperature. The resulting yellow solution (25 μL) was then dropped into the as-

prepared LIG patterns and dried in air at room temperature for 10.0 min. Then, the LIFeG nanozyme was in situ formed by a second laser-scanning on the same LIG patterns with absorbed FeCl<sub>3</sub> precursor under the same conditions. Cutting off the individual LIFeG nanozyme from the polyimide sheet using laser-cutting mode (laser power, 4.0 W; scanning speed, 830 mm/s) completes the nanozyme fabrication process. Finally, the obtained LIFeG nanozymes were repeatedly immersed into excess water, 30 min each, and washed three times, followed by vacuum drying at 60 °C for 2 h.

### *3. Characterizations*

Powder X-ray diffraction (XRD, Cu K $\alpha$  radiation) patterns were conducted with a Bruker D8 diffractometer. X-ray photoelectron spectroscopy (XPS, Al K $\alpha$  radiation) measurements were investigated by a ESCALAB 250Xi instrument (Thermo Fisher, Waltham, MA). All XPS spectra were corrected using C 1s peak at 284.8 eV as reference. The morphology of LIFeG nanozyme were observed by a scanning electron microscopy (TESCAN MIRA LMS). High resolution transmission electron microscopy (HRTEM) images were obtained using a transmission electron microscope (FEI Talos F200x). Raman spectroscopy measurements were recorded by a DXRxi Raman spectrometer (Thermo Scientific) using a 514 nm laser. The UV-Vis spectra were measured using a NanoDrop OneC Microvolume UV-vis spectrophotometer (Thermofisher). Static water contact angles were measured at room temperature on contact-angle measuring instrument (KRUSS DSA25) through the single drop technique.

#### *4. NIR Photothermal Performance of LIFeG nanozyme*

In this work, a NIR laser ( $\lambda = 808 \text{ nm}$ ) is utilized to investigate the photothermal conversion capability of LIFeG nanozyme. First, 100  $\mu\text{L}$  HAc-NaAc buffer solution (0.1 M, pH = 4.0) are added into LIFeG nanozyme, which were then horizontally exposed to a perpendicular 808 nm NIR laser illumination for continuing 5.0 min at a power density of 1.0  $\text{W}/\text{cm}^2$  and spot size of 0.5 cm in diameter. The temperature variation of the solution was continuously monitored using a digital thermometer (FOTRIC 286, China) via thermal imaging with a time interval of 5.0 s between each imaging. For comparison, the heating curves of LIG and bare PI films were also measured as a control under the same conditions. Finally, the solution on LIFeG nanozyme was exposed to an 808 nm laser for 3.0 min ON (irradiated heating) and 3.0 min OFF (natural cooling), which was repeated five times to assess the photothermal stability of LIFeG nanozyme.

#### *5. NIR light-enhanced peroxidase-like activity of LIFeG nanozyme*

The colorimetric method was employed to evaluate the peroxidase-like property of LIFeG nanozyme (0.8 cm diameter) via the catalytic oxidation of the TMB by  $\text{H}_2\text{O}_2$  in 0.1 M HAc-NaAc buffer solution (pH = 4.0), containing 0.5 mM  $\text{H}_2\text{O}_2$  and 0.5 mM TMB. In a typical test, the above TMB+ $\text{H}_2\text{O}_2$  buffer solution (100  $\mu\text{L}$ ) were added onto the surface of LIFeG nanozyme and incubated at room temperature for 5.0 min with or without NIR irradiation. Subsequently, the LIFeG nanozyme loaded with reaction solution were immersed into 100  $\mu\text{L}$  HAc-NaAc buffer and gently sonicated for 2 min. After the centrifugation to remove the slightly released nanozyme, the UV-Vis absorption spectra of the resulted solution were recorded from 400 to 800 nm on the

NanoDrop spectrophotometer. For comparison, the peroxidase-like properties of other control samples were also measured under the same conditions. The generation of  $\cdot\text{OH}$  free radicals were evaluated by methylene blue (MB) decoloration experiment under the same conditions following the same procedures mentioned above, in which 0.5 mM TMB is changed to 50  $\mu\text{M}$  MB.

#### 6. GSH Consumption

The consumption of GSH was measured by a standard Ellman's assay. Briefly, the 100  $\mu\text{L}$  GSH solution (0.4 mM GSH dissolved in 50 mM carbonate buffer, pH = 8.5) was dropped onto the surface of LIFeG nanozyme and incubated at room temperature for 10.0 min under the darkness. For NIR-treated groups, after 5.0 min co-incubation under NIR light illumination (1.0  $\text{W}/\text{cm}^2$ ), the solution was further incubated in darkness for another 5.0 min under the same conditions. Then, the LIFeG nanozyme loaded with reaction solution was transferred into 885  $\mu\text{L}$  Tris-HCl buffer (50 mM, pH 8.0). The mixtures were gently sonicated for 2.0 min and then centrifuged to remove the slightly released nanozyme. Afterward, 15  $\mu\text{L}$  DTNB solution (25 mM DTNB dissolved in 50 mM carbonate buffer, pH = 8.5) was added into the above reaction solution and incubated at room temperature for 5.0 min. The UV-Vis absorbance spectra of this mixed solution were recorded by the NanoDrop spectrophotometer. The positive and negative control experiments were performed with the same procedure as mentioned above, however, using 1.0 mM  $\text{H}_2\text{O}_2$  (Control-P) or ultrapure water (Control-N), respectively.

## 7. Bacterial Culture and Bactericidal Experiments

For bactericidal investigations, *E. coli* and *S. aureus* were used as the model Gram-negative bacteria and Gram-positive bacteria, respectively. Typically, a single colony of *E. coli* or *S. aureus* on the solid Luria-Bertani (LB) agar plate was picked up and cultured in 10 mL fresh liquid LB culture medium for 12 h on the shaker (37 °C, 180 rpm rotation). The above bacterial suspension was divided into the dark groups and the NIR light groups. For each group, 20 µL fresh bacteria suspension was mixed with 80 µL 0.1 M HAc-NaAc buffer (pH=4.0) containing 0.1 mM H<sub>2</sub>O<sub>2</sub>. In dark groups, the resulted 100 µL bacterial solution was dropped onto the surface of LIFeG nanozyme and then incubated in the darkness for 20 min at room temperature. However, the NIR light groups were first exposed to an 808 nm laser under a power density of 1.0 W/cm<sup>2</sup> for 5.0 min, followed by further incubation in the darkness for 15 min under the same conditions. Subsequently, the LIFeG nanozyme loaded with bacterial solution were immersed into 100 µL sterilized PBS buffer and gently bath-sonicated for 2 min to free the bonded bacteria from LIFeG nanozyme.<sup>1</sup> Afterward, the resulted bacteria solution was diluted 10<sup>4</sup> times, and 1.0 mL of which was spread uniformly on solid LB agar plates, followed by 24 h culture at 37 °C to generate visible bacteria colonies for counting. Control experiments were carried out in parallel without nanozyme and/or H<sub>2</sub>O<sub>2</sub>. All experiments were repeated in parallel three times.

To explore the morphology changes of both *E. coli* and *S. aureus* bacteria before and after exposure to various treatments, bacterial cells were first collected by centrifugation and washed with sterilized PBS buffer, followed by the fixation with 2.5% glutaraldehyde at 4 °C overnight

on a silicon wafer. After careful washing three times with sterilized PBS to remove residual glutaraldehyde, graded C<sub>2</sub>H<sub>5</sub>OH solutions (30, 50, 70, 80, 90, 95 and 100%) were successively employed to dehydrate the fixed bacteria for 10 min each. Finally, the resulted samples were visualized using a scanning electron microscope after vacuum drying.

Live/dead status of the bacteria after different treatments were also visually identified via the fluorescent LIVE/DEAD imaging assay using a commercial fluorescent staining solution (Solarbio cell viability kit, CA1630) containing calcein-AM (2.0 μM) and propidium iodide (4.5 μM) in 1×Assay Buffer. After different treatments, the bacteria cells were collected after being centrifugated and washed twice with the 1×Assay Buffer. Then, the bacteria cells were incubated with fluorescent staining solution for 15 min at 37 °C in the dark and then rinsed with with 1×Assay Buffer three times, followed by resuspending in 50 μL 1×Assay Buffer. Subsequently, 20 μL suspensions of the stained bacteria were dropped onto the slide and covered with a coverslip. Finally, the fluorescent images of live/dead bacterial cells were observed under a confocal laser scanning microscope (TCSsp5II, Agilent). Green fluorescence showed live bacteria and red fluorescence showed dead ones.

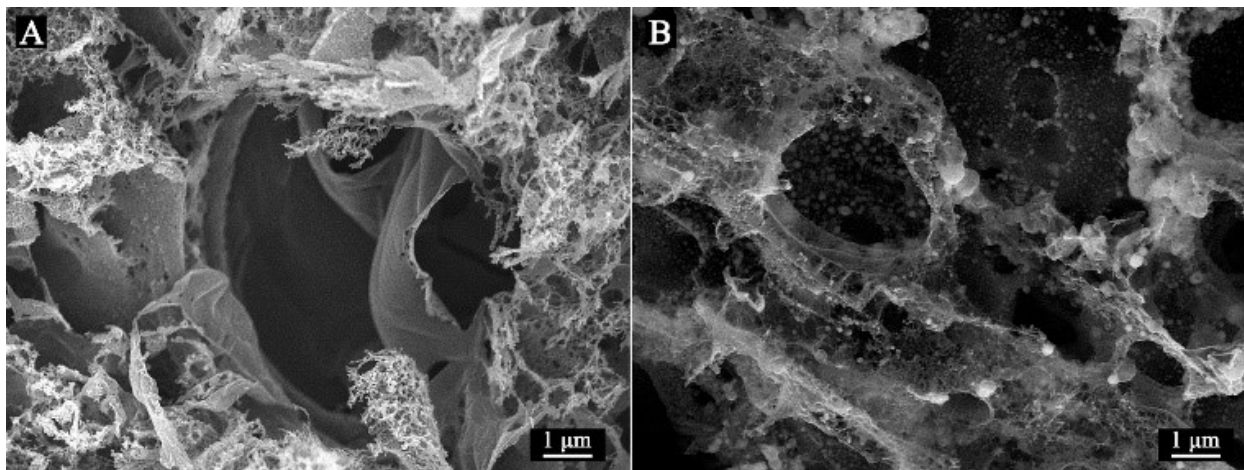


**Fig. S1.** SEM image of (A) LIG and (B) LIFeG nanozyme.

As illuminated in Fig. S1A, the surface morphology of LIG presents a 3D macroporous structure with interconnected multi-layered graphene sheets and hierarchical pores of various sizes that reaching the micron level. The observed abundant interfaces and disordered edges in the SEM image of LIG visually affirmed the high D peak in the Raman spectrum of LIG (Fig. 1B). The formation of 3D macroporous framework structure is due to the rapid gaseous evolution from the laser-induced carbonization of PI substrate under the high localized temperature,<sup>2</sup> providing a large surface area to facilitate the absorption and dispersion of  $\text{Fe}^{3+}$  precursors. From the SEM image of LIFeG nanozyme in Fig. S1B, large  $\text{Fe}_3\text{O}_4$  nanoparticles are clearly observed on the surfaces and edges of LIG sheets, which demonstrates that the diameter of these large  $\text{Fe}_3\text{O}_4$  nanoparticles is approximately 50 – 300 nm. In addition, the 3D macroporous scaffold of LIG are well-maintained in LIFeG nanozyme, benefiting for both efficient exposure of numerous  $\text{Fe}_3\text{O}_4$  active sites and better diffusion of  $\text{H}_2\text{O}_2$ ,  $\cdot\text{OH}$ , and even bacteria.

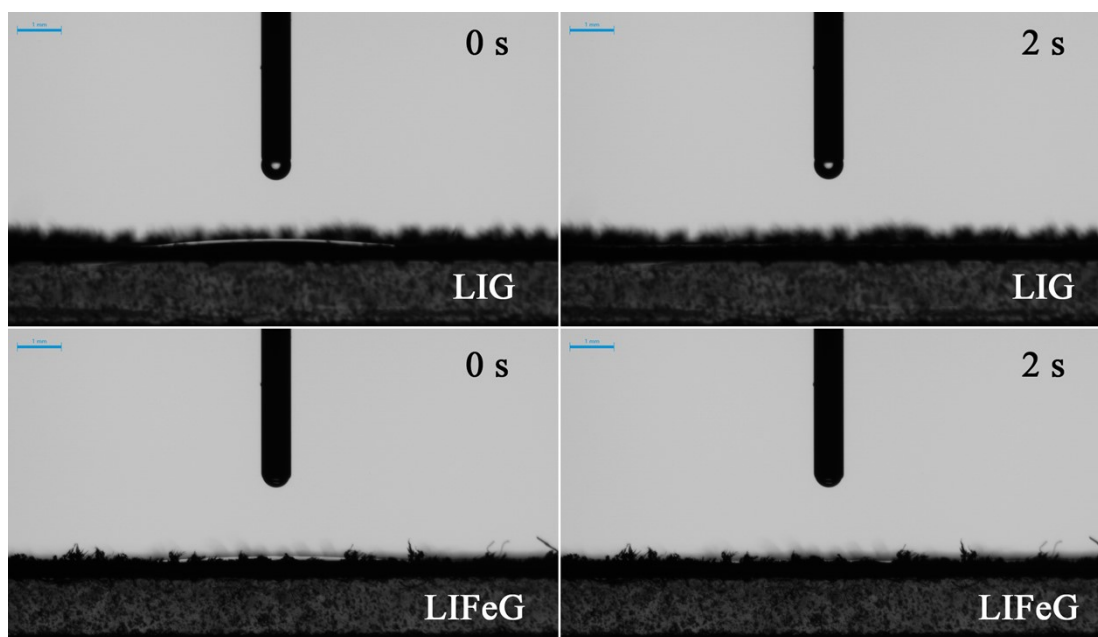


**Fig. S2.** Hydrophilicity of LIG and LIFeG nanozyme.

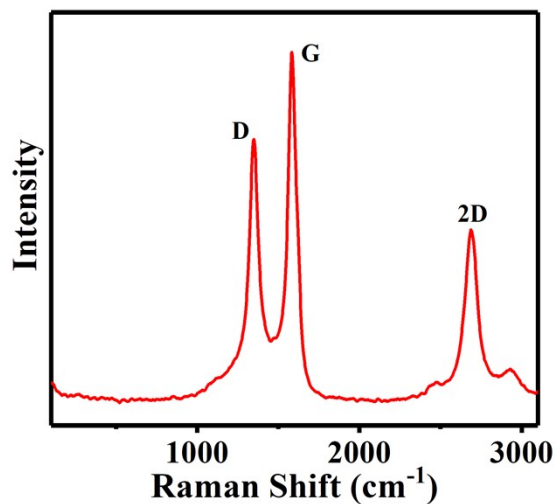


**Fig. S3.** Raman spectrum of LIG.

In the Raman spectrum of LIG (Fig. S3), three typical scattering peaks located at around 1350, 1580, and 2690  $\text{cm}^{-1}$  can be perfectly indexed to the D band, G band, and 2D band of graphene structure.<sup>2</sup> Whereas the D band is arised from the structural defects or edge condition in the graphitic disorders structure, G band is related to planar vibrations of graphitic  $\text{sp}^2$  carbon atoms, and 2D band is originated from second-order zone-boundary phonons. Comparative analysis of the  $I_D/I_G$  data in Fig. S3 and Fig. 1B showed that the LIFeG nanozyme possessed a higher  $I_D/I_G$  ratio (0.86) than LIG (0.75), indicating the generation of defective structures in LIG, which is benefit for improving the charge/mass transfer efficiency of the catalytic LIFeG nanozyme.<sup>3</sup>

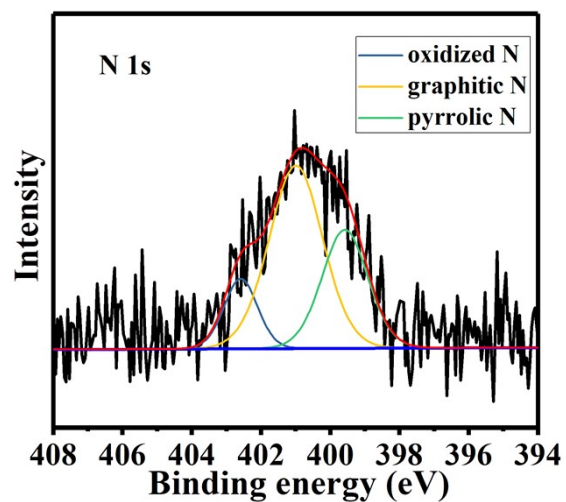


**Fig. S4.** High resolution N 1s XPS spectrum of LIFeG nanozyme.

The N 1s core level XPS spectrum of LIFeG nanozyme (Fig. S4) can be divided into three components centred at 399.6 eV (pyrrolic N), 401.0 eV (graphitic N), and 402.6 eV (oxidized N) species, implying that the as-prepared LIFeG nanozyme consisted of N-dopant in the LIG carbon structure.

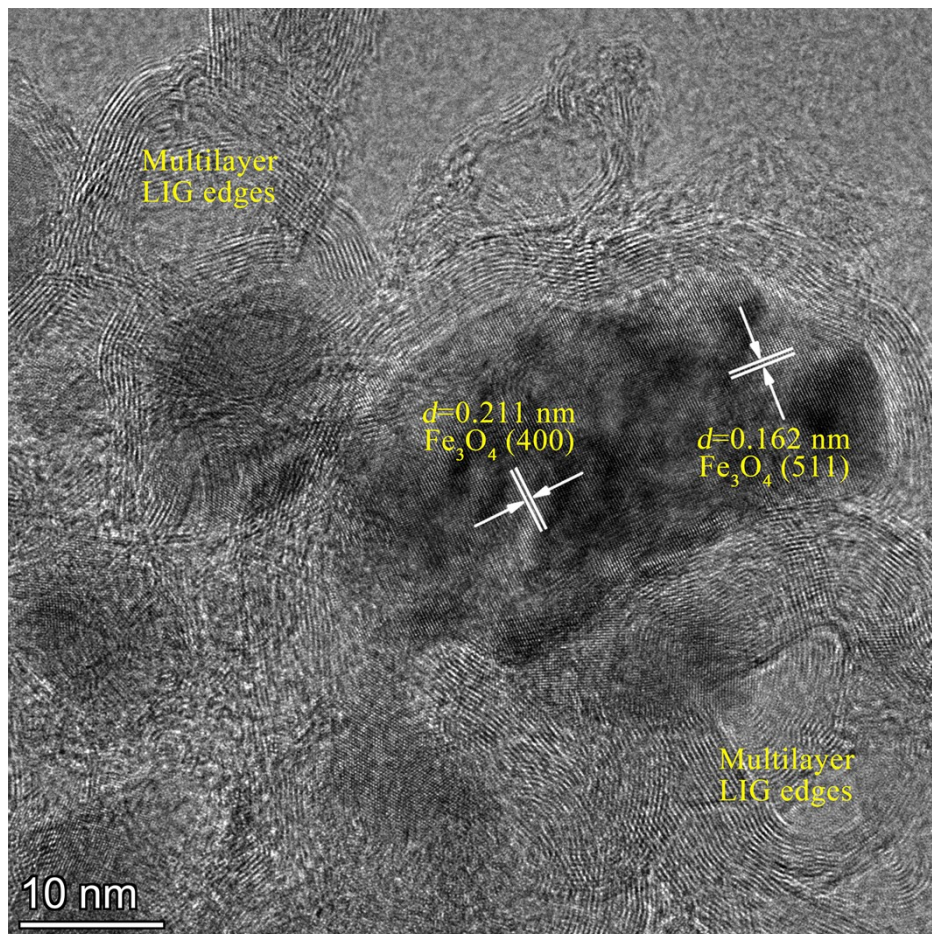


**Fig. S5.** HRTEM image of LIFeG nanozyme.

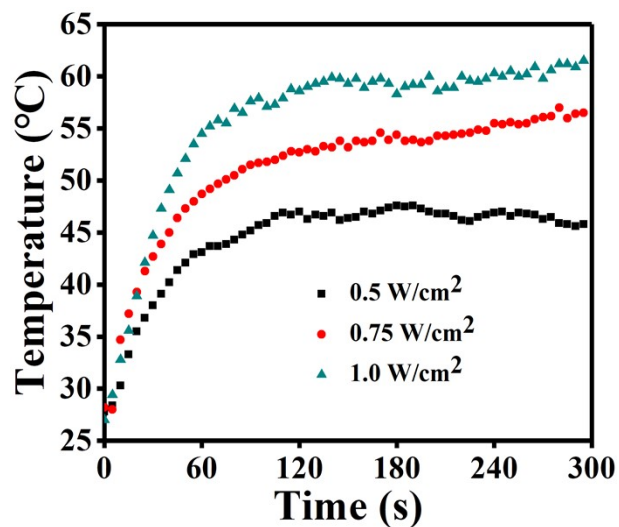


**Fig. S6.** Temperature change curves of 100  $\mu\text{L}$  HAC-NaAc buffer solution on LIFeG nanozyme under different NIR laser power density as a function of irradiation time.

As shown in the temperature change curves (Fig. S6), the temperature ramping rate of the solution on LIFeG nanozyme raised obviously with the elevation of NIR laser power, suggesting that the photothermal conversion process of LIFeG nanozyme could be controlled by reasonably adjusting the NIR laser power.

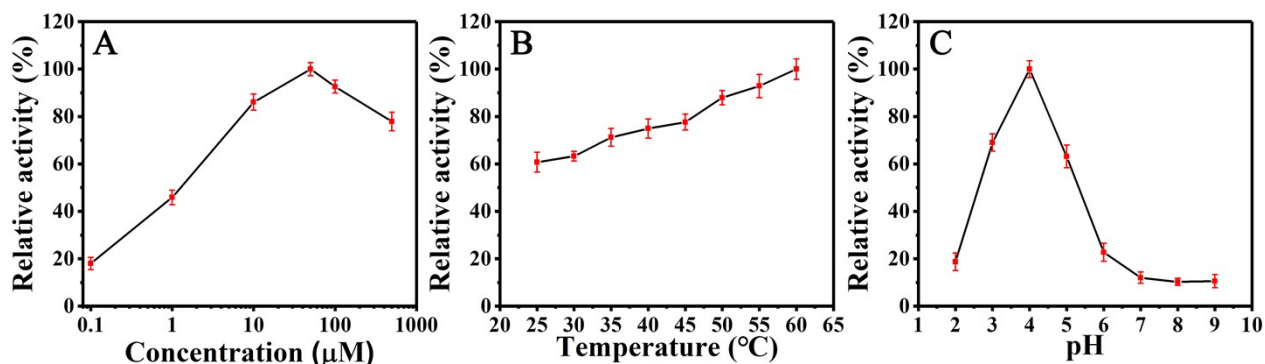


**Fig. S7.** Influence of (A) Fe<sup>3+</sup> precursor concentration, (B) temperature, and (C) pH on the POD-like activity of LIFeG nanozyme.

The peroxidase-mimic activity of LIFeG nanozyme was dependent on the concentration of Fe<sup>3+</sup> precursor (Fig. S7), showing the optimal peroxidase-like activity at 50 μM Fe<sup>3+</sup> precursor. Furthermore, the influence of temperature and pH on the peroxidase-mimic activity of LIFeG nanozyme was also investigated (Fig. S7B,C). It was found that the POD-mimic catalytic activity of LIFeG nanozyme increased with the elevating of pH from 2.0 to 4.0, and then decreased gradually in the pH range from 4.0 to 7.0, while LIFeG nanozyme shows an enhanced peroxidase-mimicking activity at increased temperatures as high as 60 °C, suggesting its high thermal stability and good feasibility in photothermal-enhanced nanozyme catalysis.

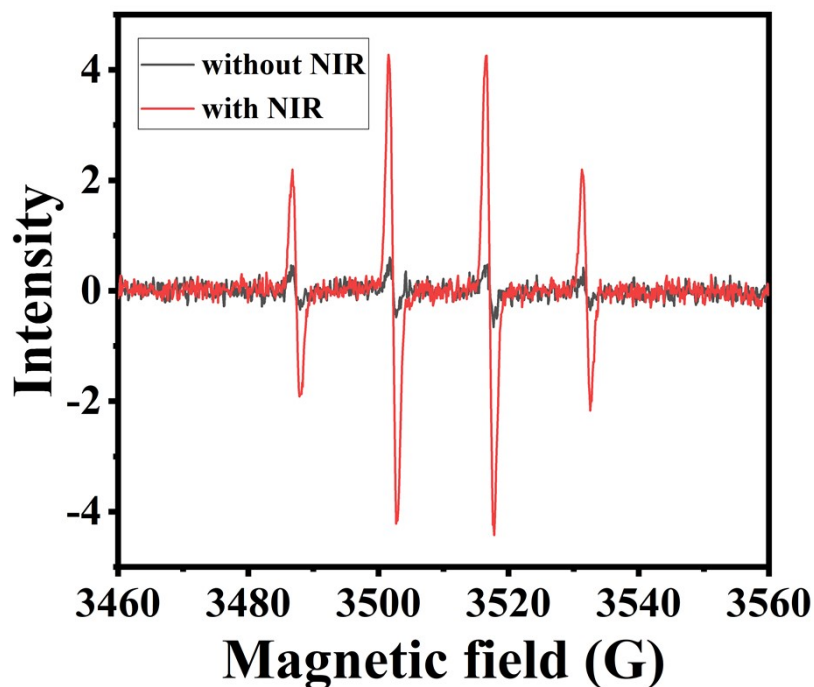


**Fig. S8.** ESR spectra of  $\cdot\text{OH}$  trapped by DMPO upon LIFeG+ $\text{H}_2\text{O}_2$  treatment without or with NIR irradiation ( $1.0 \text{ W/cm}^2$ , 5 min).

To further confirm the generation of  $\cdot\text{OH}$  in the presence of both LIFeG nanozyme and  $\text{H}_2\text{O}_2$  with or without NIR irradiation, spin trapping agent 5,5-dimethyl-1-pyrroline-N-oxide (DMPO) was used to capture free radicals for in situ electron spin resonance (ESR) measurements. As shown in Fig. S8, both the LIFeG+ $\text{H}_2\text{O}_2$  group and LIFeG+ $\text{H}_2\text{O}_2$ +NIR group exhibited the typical 1:2:2:1 characteristic signal, which indicates that the LIFeG nanozyme catalyzes  $\text{H}_2\text{O}_2$  to generate hydroxyl radicals ( $\cdot\text{OH}$ ). Moreover, the characteristic peak intensity of LIFeG+ $\text{H}_2\text{O}_2$  group with NIR irradiation was much stronger than that without NIR irradiation, which also confirms the promotion of  $\cdot\text{OH}$  generation under NIR irradiation.

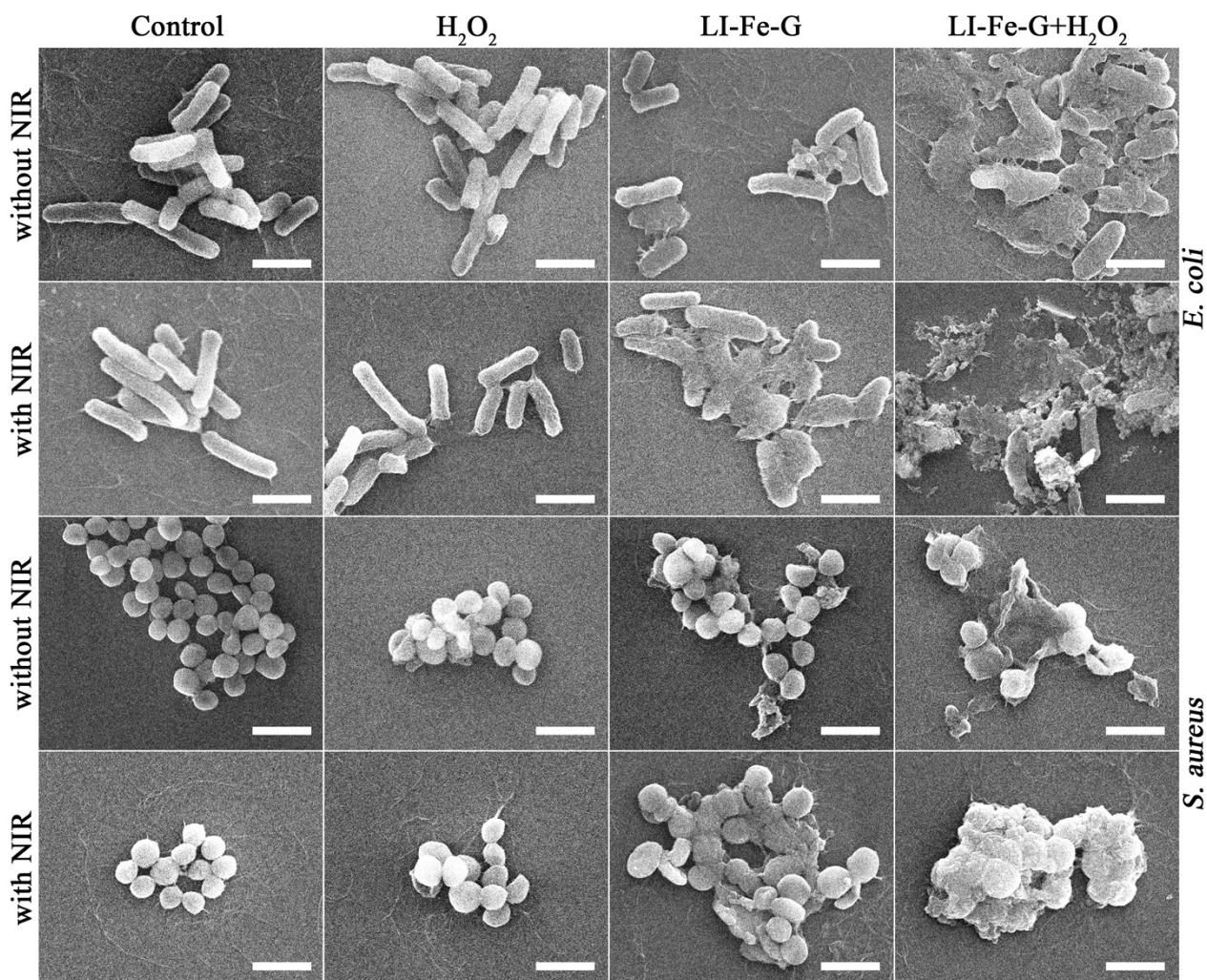


**Fig. S9.** SEM images of *E. coli* and *S. aureus* after different treatments. Scale bar, 2.0  $\mu\text{m}$ .

To further demonstrate the bactericidal behavior of LIFeG nanozyme, the morphology and integrity change of *E. coli* and *S. aureus* bacterial cells upon different treatments was assessed by SEM images. It can be seen from Fig. S9 that the bacterial morphology of the bacteria cells in the control groups is smooth with an intact cell integrity whether exposed to NIR light or not. Similarly, the incubation with H<sub>2</sub>O<sub>2</sub> alone caused no obvious damage toward bacteria cells. After the exposure to H<sub>2</sub>O<sub>2</sub>+NIR group, the surface of bacteria cell membrane slightly adhered together and wrinkled, however, with negligible integrity change. In comparison, the cell integrities of

some bacteria are obviously damaged in the LIFeG-treated group, indicating that LIFeG nanozyme itself has a certain killing effect on bacterial cells. Whereas, apparent deformation/collapse and even fusion of most bacterial cells was observed in the LIFeG+NIR and LIFeG+H<sub>2</sub>O<sub>2</sub> groups. As expected, almost all the bacteria cells treated with LIFeG+H<sub>2</sub>O<sub>2</sub> under NIR irradiation exhibited the most severe damage of cell integrity, causing the complete loss of cell morphology along with intracellular matrix leakage from bacteria.

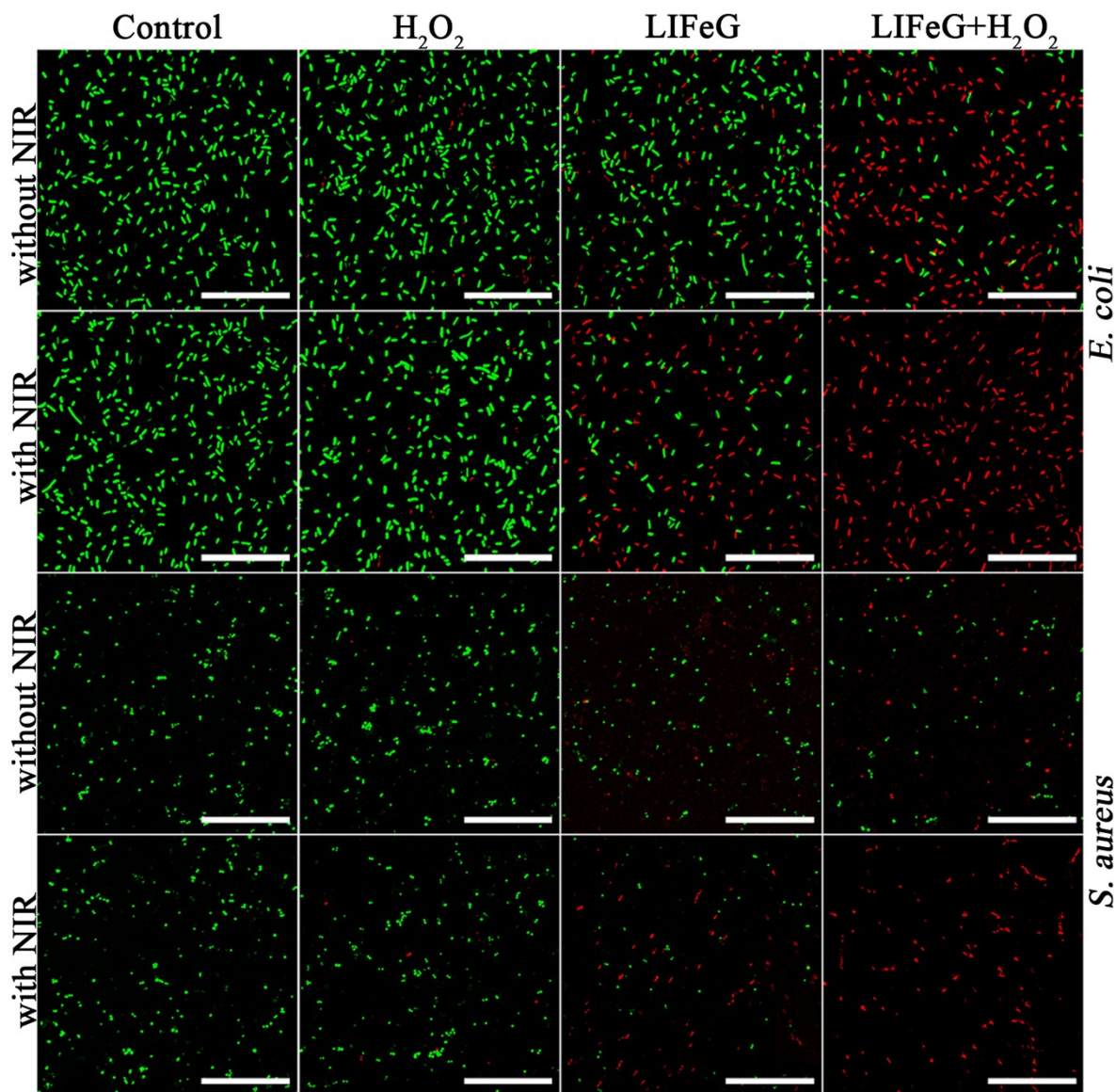


**Fig. S10.** Fluorescence images of live (green) and dead (red) bacterial cells after various treatments. Scale bar, 25  $\mu\text{m}$ .

The results of live/dead cell double staining test further confirmed the synergistic bactericidal performance of the LIFeG nanozyme under NIR irradiation. As shown in Fig. S10, almost all *E. coli* and *S. aureus* cells in the control group and H<sub>2</sub>O<sub>2</sub>-treated group without or with NIR illumination exhibit bright green fluorescence, manifesting good viability and membrane integrity of bacterial cells. However, a small number of dead bacteria with red fluorescence were

observed in the LIFeG-treated group, which clearly demonstrated that LIFeG alone had limited bactericidal action on the bacteria. In contrast, a majority of bacteria cells reveal red fluorescent in LIFeG+H<sub>2</sub>O<sub>2</sub> group, illustrating that the POD-like activity of LIFeG nanozyme had excellent bactericidal efficiency. Under NIR irradiation, the green fluorescence in LIFeG group decreased obviously, while all bacteria in LIFeG+H<sub>2</sub>O<sub>2</sub> group were stained with red fluorescence, indicating a significantly enhanced bactericidal effect from the catalytic-photothermal synergetic strategy.

## References

1. M. G. Stanford, J. T. Li, Y. Chen, E. A. McHugh, A. Liopo, H. Xiao and J. M. Tour, *ACS Nano*, 2019, **13**, 11912–11920.
2. J. Lin, Z. Peng, Y. Liu, F. Ruiz-Zepeda, R. Ye, E. L. G. Samuel, M. J. Yacaman, B. I. Yakobson and J. M. Tour, *Nat. Commun.*, 2014, **5**, 5714.
3. H. Sun, Y. Zhou, J. Ren and X. Qu, *Angew. Chem. Int. Ed.*, 2018, **57**, 9224-9237.